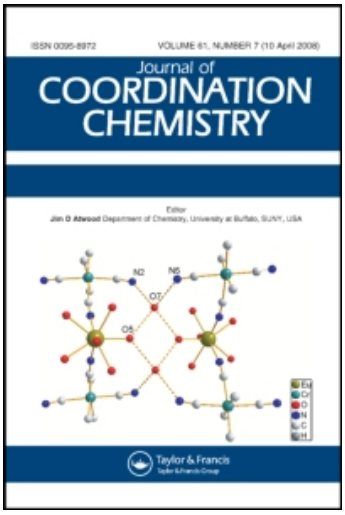

Journal of Coordination Chemistry
Publication details, including instructions for authors and subscription information:
http://www.informaworld.com/smpp/title~content=t713455674

Syntheses, crystal structures and magnetic properties of two new ionic pair complexes with well-separated columnar stack structures based on

Chunlin Ni[ab]; Yiping Zheng[b]; XueYi Le[a]
[a] Department of Applied Chemistry, College of Science, South China Agricultural University, 510642 Guangzhou, P.R. China [b] Centre of Inorganic Functional Materials, South China Agricultural University, 510642 Guangzhou, P.R. China

To cite this Article Ni, Chunlin , Zheng, Yiping and Le, XueYi(2006) 'Syntheses, crystal structures and magnetic properties of two new ionic pair complexes with well-separated columnar stack structures based on ', Journal of Coordination Chemistry, 59: 10, 1173 — 1182
To link to this Article: DOI: 10.1080/00958970500448309
URL: http://dx.doi.org/10.1080/00958970500448309

Journal of Coordination Chemistry
Vol. 59, No. 10, 10 July 2006, 1173–1182

Syntheses, crystal structures and magnetic properties of two new ionic pair complexes with well-separated columnar stack structures based on $Ni(mnt)_2^-$

CHUNLIN NI*†‡, YIPING ZHENG‡ and XUEYI LE†

†Department of Applied Chemistry, College of Science,
South China Agricultural University,
510642 Guangzhou, P.R. China
‡Centre of Inorganic Functional Materials, South China Agricultural University,
510642 Guangzhou, P.R. China

(*Received 13 May 2005; in final form 1 August 2005*)

The crystal structures of two new ion-pair complexes, [DiClBzPy][Ni(mnt)$_2$] (**1**), and [DiClBzQl][Ni(mnt)$_2$] (**2**), ([DiClBzPy]$^+$ = 1-(2′,4′-dichlorobenzyl)-pyridinium, [DiClBzQl]$^+$ = 1-(2′,4′-dichlorobenzyl)-quinolinium, and mnt^{2-} = maleonitriledithiolate) were determined. The $Ni(mnt)_2^-$ anions and cations of **1** and **2** stack into well-segregated columns in the solid state; the Ni(III) ions form a 1D zigzag chain within a $Ni(mnt)_2^-$ column through Ni···S, S···S, Ni···Ni or $\pi\cdots\pi$ interactions. For **2**, the anion–anion, anion–cation and cation–cation contacts play important roles in packing and stabilization. The variable temperature magnetic susceptibilities of **1** and **2** in the 75–298 K range have been interpreted in terms of simple dimer approximation ($H = 2JS_AS_B$). The results reveal that both complexes exhibit strong antiferromagnetic interactions with the fitting value $g = 2.12$ and $J = -298.2\,cm^{-1}$ for **1**, $g = 2.17$ and $J = -218.4\,cm^{-1}$ for **2**.

Keywords: Bis(maleonitriledithiolate)nickelate(III); Pyridinium derivative; Quinolinium derivative; Crystal structure; Magnetic property

1. Introduction

Since the first ferromagnet containing $Ni(mnt)_2^-$ (mnt^{2-} = maleonitriledithiolate) ion, $NH_4\cdot Ni(mnt)_2\cdot H_2O$, was discovered by Coomber *et al.*, the investigation of mnt^{2-} transition metal complexes has become a fascinating subject in the field of molecule-based magnetic materials [1–6]. In the course of our investigations on these complexes, we have developed a new class of ion-pair complexes $[RbzPy]^+[Ni(mnt)_2]^-$ ([RbzPy]$^+$ = derivatives of benzylpyridinium) which exhibit versatile magnetic properties such as ferromagnetic ordering at low temperature, magnetic transitions from ferromagnetic coupling to diamagnetism, meta-magnetism and spin-Peierls-like

*Corresponding author. E-mail: scauchemnicl@163.com

Journal of Coordination Chemistry
ISSN 0095-8972 print: ISSN 1029-0389 online © 2006 Taylor & Francis
DOI: 10.1080/00958970500448309

transitions [7–13]. In these ion-pair complexes, the prominent structural feature is that the $Ni(mnt)_2^-$ ions and $[RbzPy]^+$ cations stack into well-segregated columns in the solid state; the topology and size of the countercation in $Ni(mnt)_2^-$ complexes play important role in controlling the stacking pattern of anions and cations, further influencing the magnetic properties of these complexes. To widen the scope of our research and obtain more information on the influence of counteraction on the stacking pattern and magnetic properties of $Ni(mnt)_2^-$ complexes, in this article we describe the syntheses, crystal structures and magnetic behavior of two new ion-pair complexes, [DiClBzPy][Ni(mnt)$_2$] (**1**), and [DiClBzQl][Ni(mnt)$_2$] (**2**), ($[DiClBzPy]^+$ = 1-(2′,4′-dichlorobenzyl)-pyridinium, $[DiClBzQl]^+$ = 1-(2′,4′-dichlorobenzyl)-quinolinium, and mnt^{2-} = maleonitriledithiolate). $Ni(mnt)_2^-$ complexes containing disubstituted benzyl-pyridinium or quinolinium cations have rarely been reported [11].

2. Experimental

2.1. *Materials*

2,4-Dichlorobenzyl bromide, pyridine and quinoline were purchased from Aldrich and used without further purification. [1-(2′,4′-dichlorobenzyl)]-pyridinium ([DiClBzPy]Br) bromide and ([DiClBzQl]Br) [1-(2′,4′-dichlorobenzyl)]-quinolinium bromide ([DiClBzQl]Br) were prepared by the literature method [14]. Disodium maleonitriledithiolate (Na_2mnt) was synthesized by a published procedure, and a similar method for preparing $[Bu_4N]_2[Ni(mnt)_2]$ was used to prepare $[DiClBzPy]_2[Ni(mnt)_2]$ and $[DiClBzQl]_2[Ni(mnt)_2]$ [15].

2.2. *Preparation of 1 and 2*

[DiClBzPy][Ni(mnt)$_2$] was synthesized as follows. An acetone solution (10 cm^3) of I_2 (160 mg, 0.62 mmol) was slowly added to an acetone solution (50 cm^3) of $[DiClBzPy]_2[Ni(mnt)_2]$ (817 mg, 1 mmol) and the mixture was stirred for 2 h. MeOH (90 cm^3) was then added, and the mixture allowed to stand overnight; 521 mg of black micro-crystals formed and were filtered off, washed with MeOH and dried in vacuum (yield: 90.1%). Anal. Calcd for $C_{20}H_{10}N_5NiCl_2S_4$: C, 41.55; H, 1.74; N, 12.13. Found: C, 41.23; H, 1.88; N, 12.01%. ESI-MS (m/z): 238.1, $[DiClBzPy - H]^+$; 338.1, $[Ni(mnt)_2 + H]^+$.

The procedure for preparing [DiClBzQl][Ni(mnt)$_2$] is similar to that for **1**. Yield: 82.5%. Anal. Calcd for $C_{24}H_{12}N_5NiCl_2S_4$: C, 45.88; H, 1.92; N, 11.52. Found: C, 46.02; H, 2.20; N, 11.41%. ESI-MS (m/z): 288.1, $[DiClBzQl - H]^+$; 337.9, $[Ni(mnt)_2 + H]^-$.

Black single crystals suitable for X-ray structure analysis were obtained by evaporating MeCN and *i*-PrOH (v/v = 1 : 1) mixed solutions of **1** and **2** over about two weeks at room temperature.

2.3. *Physical measurements*

Elemental analyses for C, H, N were determined on a Model 240 Perkin Elmer CHN analytical instrument. IR spectra (KBr pellets) were obtained with

a VECTORTM 22 FT-IR (400–4000 cm^{-1}) spectrophotometer. Electronic spectra were recorded on a Shimadzu UV-3100 spectrophotometer. All solution concentrations were ca 10^{-5} mol dm^{-3} in CH_3CN. The electrospray mass spectra [ESI–MS] were determined on a Finnigan LCQ mass spectrograph (sample concentration ca 1.0 mmol dm^{-3}). Magnetic susceptibility measurements were carried out down to liquid nitrogen temperature with a CAHN-2000 Faraday type magnetometer; diamagnetic corrections for the constituent atoms were made with Pascal's constants.

2.4. *Single-crystal X-ray structure determination*

Measurements of complexes **1** and **2** were performed on a Smart APEX CCD area detector using graphite-monochromated Mo-Kα radiation ($\lambda = 0.71073$ Å) in the ω scan mode within the angular range $1.8 < \theta < 25.0^\circ$ for **1** and $1.9 < \theta < 25.0^\circ$ for **2**. Space group, lattice parameters, and other relevant information are listed in table 1. The structures were solved by direct methods and refined on F^2 by full-matrix least-squares, employing Bruker's SHELXTL [16]. All non-hydrogen atoms were refined with anisotropic thermal parameters. All H atoms were placed in calculated positions,

Table 1. Crystallographic data of **1** and **2**.

Complex	**1**	**2**
Empirical formula	$C_{20}H_{10}N_5NiCl_2S_4$	$C_{24}H_{12}N_5NiCl_2S_4$
Formula weight	578.18	628.24
Description	Black block	Black block
Crystal size (mm^3)	$0.4 \times 0.3 \times 0.2$	$0.3 \times 0.2 \times 0.2$
Temperature (K)	293(2)	293(2)
Wavelength (Å)	0.71073	0.71073
Space system	Triclinic	Triclinic
Space group	$P\bar{1}$	$P\bar{1}$
Unit cell dimensions		
a (Å)	7.068(1)	7.157(1)
b (Å)	12.768(2)	13.250(2)
c (Å)	14.732(2)	14.635(2)
α (°)	65.06(1)	98.18(1)
β (°)	80.03(1)	101.58(1)
γ (°)	76.49(1)	102.35(1)
Volume ($Å^3$)	1167.9(3)	1302.9(3)
Z	2	2
Density (calculated, g cm^{-3})	1.644	1.601
Absorption coefficient (mm^{-1})	1.436	1.295
$F(000)$	582	634
Absorption correction	Empirical	Empirical
Max. and min. transmission	0.75 and 0.66	0.77 and 0.68
θ range (°)	$1.8 < \theta < 25.0$	$1.9 < \theta < 25.0$
Refinement method	Full-matrix least-squares on F^2	Full-matrix least-squares on F^2
Reflection collected	5864	6407
Independent reflection (R_{int})	4054(0.038)	4497(0.036)
Data, restraints, parameters	4054, 0, 289	4497, 0, 325
Goodness-of-fit on F^2	1.031	1.012
R_1, wR_2 ($I > 2\sigma(I)$)	0.0527, 0.0853	0.0488, 0.0800
R_1, wR_2 (all data)	0.1130, 0.0933	0.0794, 0.0862
Largest diff. peak and hole (e $Å^{-3}$)	0.43 and −0.35	0.47 and −0.27

assigned fixed isotropic displacement parameters 1.2 times the equivalent isotropic U value of the attached atom, and allowed to ride on their respective parent atoms.

3. Results and discussions

3.1. *Description of the structures*

An ORTEP drawing of complex **1** with non-hydrogen atomic labeling of the asymmetric unit is shown in figure 1. The unit cell is comprised of a $Ni(mnt)_2^-$ anion and $[DiClBzPy]^+$, and the Ni(III) ion is coordinated by four S atoms of two mnt^{2-} ligands and exhibits the expected square-planar coordination geometry. The CN groups of $Ni(mnt)_2^-$ are slightly tipped out of the plane; the deviations from the plane are 0.0670 Å for N(1), 0.1074 Å for N(2), −0.3138 Å for N(3) and −0.2593 Å for N(4). The average Ni–S bond distance is 2.143(2) Å, and the average S–Ni–S bond angle within the five-membered rings is 90.00(7)°, comparing well with those found in $Ni(mnt)_2^-$ complexes [17]. The $[DiClBzPy]^+$ cation adopts a conformation where both the phenyl and pyridine rings are twisted relative to the C(14)–C(15)–N(5) reference plane. The deviations of the Cl atoms from the phenyl ring plane are −0.0632 Å for Cl(1) and 0.0874 Å for Cl(2). The dihedral angles that the pyridine ring and the phenyl ring make with the C(14)–C(15)–N(5) reference plane are 109.8° and 64.3°, respectively. The phenyl ring and the pyridine ring make a dihedral angle of 80.6°. In complex **1** the $Ni(mnt)_2^-$ ions and $[DiClBzPy]^+$ cation stack into well-segregated columns along the crystallographic a-axis (figure 2). In an anionic stacking column, the Ni···Ni distances alternate between 3.993 Å (A–B) and 4.303 Å (A′–B), and the nearest Ni···S and S···S distances are 3.437 Å (A–B) and 3.826 Å

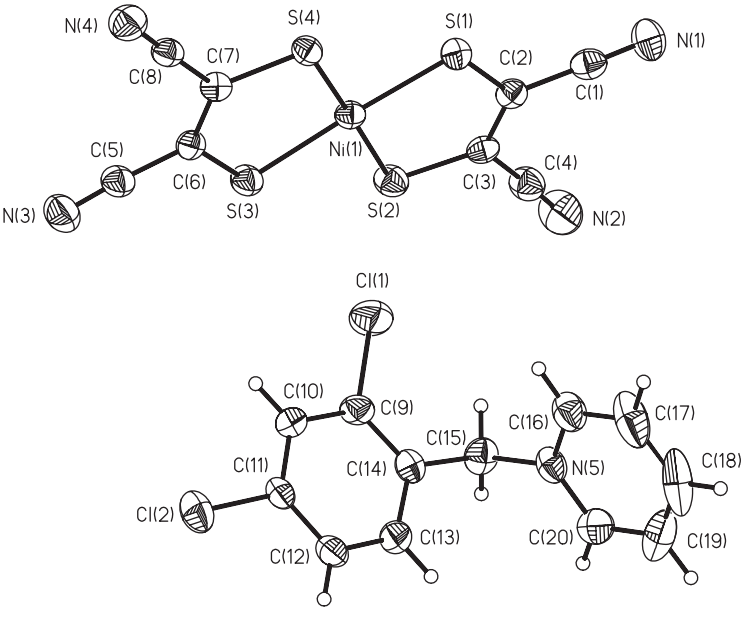

Figure 1. ORTEP plot (30% probability ellipsoids) showing the molecule structure of **1**.

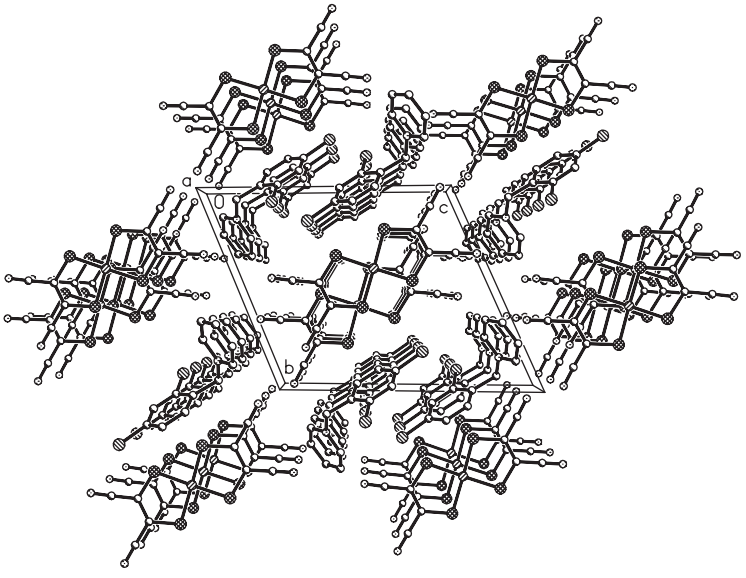

Figure 2. The packing diagram of a unit cell for **1** as viewed along *a*-axis.

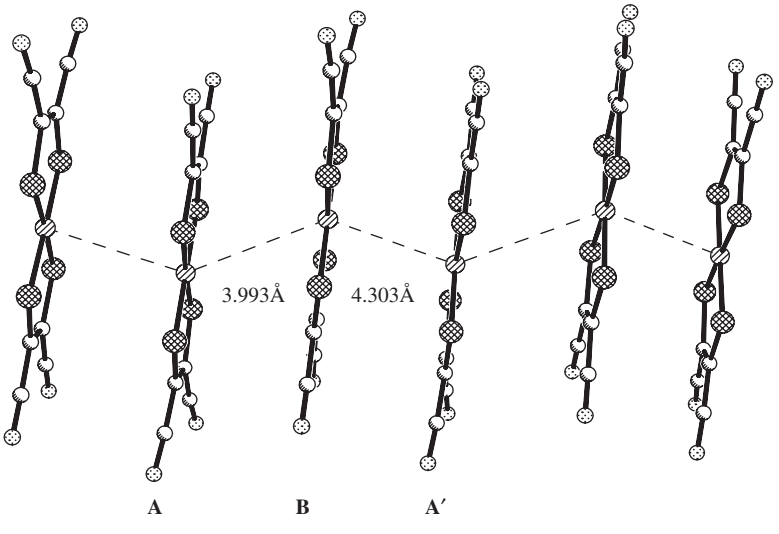

Figure 3. Side view of the anion stack of **1** showing the alternating, linear-chain of $[Ni(mnt)_2]^-$.

(A′–B), respectively. The closest Ni···Ni separation between anion columns is 12.768 Å, significantly longer than Ni···Ni separation within a column. Therefore, each $Ni(mnt)_2^-$ anion can be considered as a one-dimensional magnetic chain in an alternating zigzag fashion(A–B–A′) by virtue of intermolecular Ni···S, S···S or $\pi\cdots\pi$ interactions (figure 3). The significant interaction in adjacent cations is a p–π interaction between chlorine of one phenyl ring and another phenyl ring (the contact distance of Cl(2) atom to the center of neighboring benzene ring

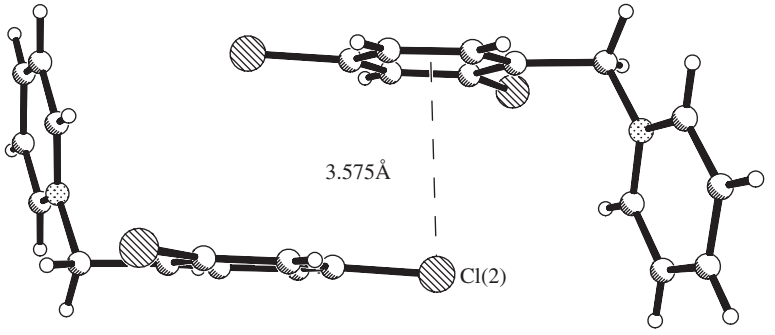

Figure 4. The intermolecular contact in two neighboring cations of **1**.

Table 2. Selected bond parameters and intermolecular contacts for **1** and **2**.

Compound	**1**	**2**
Bond distances (Å)		
Ni(1)–S(1)	2.140(2)	2.148(1)
Ni(1)–S(2)	2.138(2)	2.137(1)
Ni(1)–S(3)	2.143(2)	2.144(1)
Ni(1)–S(4)	2.153(2)	2.152(1)
S(1)–C(2)	1.719(6)	1.706(4)
S(2)–C(3)	1.704(6)	1.706(4)
S(3)–C(6)	1.713(6)	1.703(4)
S(4)–C(7)	1.717(6)	1.713(4)
Bond angles (°)		
S(1)–Ni(1)–S(2)	92.38(7)	92.54(4)
S(1)–Ni(1)–S(4)	88.85(7)	89.55(4)
S(3)–Ni(1)–S(4)	92.58(7)	92.72(4)
S(2)–Ni(1)–S(3)	86.18(8)	85.21(4)
Intrachain distances (Å)		
Ni···Ni (nearest separation)	3.993(A–B), 4.303(A′–B)	4.012(A–B), 4.195(A′–B)
Ni···S	3.437(A–B), 3.650(A′–B)	3.498(A–B), 3.666(A′–B)
S···S	3.826(A–B), 3.959(A′–B)	3.920(A–B), 3.956(A′–B)
Interchain distances (Å)		
Ni···Ni (nearest separation)	12.768	11.212

is 3.575 Å) (figure 4), and the cation–cation interactions give rise to a cation column with a rectangular channel extending along the crystallographic *a*-axis.

Complex **2** is isostructural with **1**; the bond parameters in the anionic $Ni(mnt)_2^-$ entry and intermolecular contacts are presented in table 2. Compared with the values for **1**, the nearest separations of Ni···Ni, Ni···S and S···S are longer than for **1**, and it is possible that the intermolecular interaction in a $Ni(mnt)_2^-$ column is less than that in **1**. Two intramolecular and two intermolecular hydrogen bonds between anions and cations were observed in the crystal structure as shown in figure 5. The intramolecular contact between N(4) and C(17) is 3.322(6) and the hydrogen atom associated with the atom has the following contacts with N(4)···H(17) 2.530 Å. The intermolecular contacts are N(2) with the C(16) $(-x+1, -y+1, -z)$ atom at 3.427(6) Å and N(1) with the C(22) $(-x, -y, -z)$ at 3.518(6) Å. The hydrogen atoms associated with these

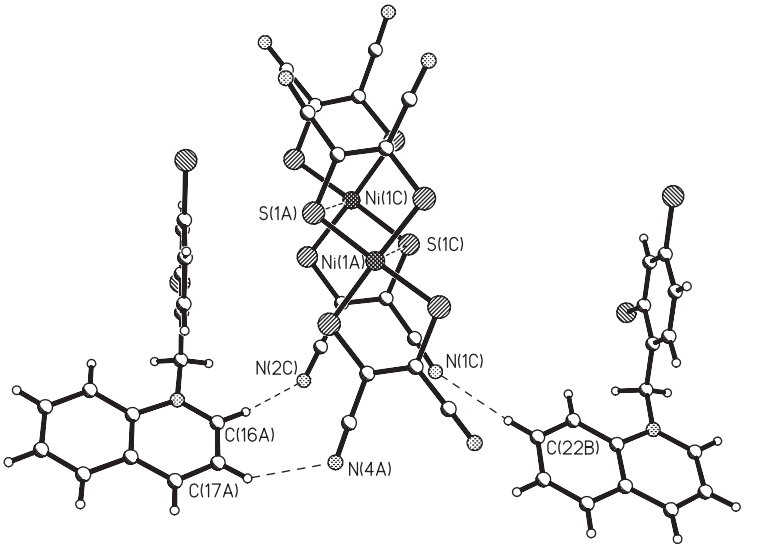

Figure 5. The intermolecular contacts between anions and cations of **2**.

atoms have contacts with N(2)···H(16) 2.530 Å and N(1)···H(22) 2.620 Å. The anion–anion, anion–cation and cation–cation contacts play important roles in the packing and stabilization of **1**.

3.2. *Infrared spectra, electronic absorption spectra and electrospray mass spectra*

The main infrared and electronic absorption spectral bands of **1** and **2** are listed in table 3. In the IR spectrum of complex **1**, the bands at 3060.6, 2925.7 and 2845.7 cm^{-1} are assigned to the stretching vibrations of C–H in the aromatic ring and methylene. The very strong ν(C≡N) band is at 2203.9 cm^{-1}. The ν(C=N), ν(C=C) bands for the pyridine ring and phenyl ring are at 1632.1(m), 1592.6(s), 1563.8(m) and 1541.7(s) cm^{-1}. ν(C=C) of mnt^{2-} is at 1444.6(s) cm^{-1}. The bands at 677.4(m) and 595.8(w) cm^{-1} originate from ν(C–Cl). The infrared spectra of **2** are similar to these of **1** (table 3). Solution electronic spectra of **1** and **2** were measured in CH_3CN in the UV-Vis region (230–1200 nm), and four strong bands and two weak bands are attributed to the anionic portions of these compounds. The characteristic bands at 861.0, 477.0, 312.0 and 269.0 nm for **1**, and 858.0, 478.0, 314.0, 270.0 nm for **2** are assigned as $L(\pi) \rightarrow M$, $L(\sigma) \rightarrow M$, $L^* \rightarrow L$ and $L(\sigma) \rightarrow M$, basically similar to $[(n\text{-}C_4H_9)_4N][Ni(mnt)_2]$ [18]. The negative-ion and positive-ion ESI-MS spectra of **1** and **2** in MeCN solution show that the mass spectrum is dominated by the 337.9 peak which is due to $[Ni(mnt)_2 + H]^-$, the peaks at 238.1 and 288.1 are assigned to $[DiClBzPy - H]^+$ and $[DiClBzQl - H]^+$, respectively.

3.3. *Magnetic susceptibilities*

Variable-temperature magnetic susceptibility measurements of **1** and **2**, performed on their crystalline samples from 298 to 75 K, are shown in figure 6 in the form of $\chi_M T$ *versus* T. Corrections for diamagnetism of the complexes are estimated from

Table 3. The main UV-Vis (CH_3CN) and main infrared spectral absorptions of **1** and **2**.

Complex	UV-Vis [λ(nm) (ε $M^{-1}\,cm^{-1}\,10^4$)]	IR (cm^{-1})
1	1161.0(0.019)	3082.4(w), 3060.6(w), 2925.7(w)
	861.0(0.722)	2845.7(w), 2203.9(s), 1632.1(m)
	597.0(0.040)	1592.6(s), 1563.8(m), 1541.7(s)
	477.0(0.227)	1474.8(s), 1444.6(m), 677.4(m)
	312.0(2.918)	595.8(m)
	269.0(3.369)	
2	1179.0(0.026)	3077.8(w), 3057.4(w), 2922.5(w)
	858.0(0.763)	2834.7(w), 2204.6(s), 1626.8(m)
	598.0(0.042)	1590.7(s), 1562.4(m), 1530.1(s)
	478.0(0.249)	1470.7(s), 1447.9(m), 680.7(m)
	314.0(3.891)	599.2 (m)
	270.0(3.579)	

Pascal's constants to be -260.18×10^{-6} emu mol^{-1} for **1**, and -282.71×10^{-6} emu mol^{-1} for **2**. In the whole temperature range, **1** and **2** show similar magnetic behavior. At 298 K, the $\chi_M T$ values of **1** and **2** are 0.166 emu K mol^{-1} and 0.364 emu K mol^{-1}, respectively, less than the calculated spin-only value of 0.375 emu K mol^{-1} for a system comprised of non-interacting $g=2$, $S=1/2$ spin sites, and the value of **1** is significantly less than that of **2**, indicating a significant antiferromagnetic coupling contribution which is stronger for **1** than for **2**. When the system cools, the values of $\chi_M T$ decreases quickly to 0.0105 emu K mol^{-1} at 148 K for **1**, and 0.0135 emu K mol^{-1} at 125 K for **2**, then slowly drops to zero at 75 K. The Ni···Ni distance of anions A′ and B is larger than that for anions A and B in nickel(III) ion chains, thus, the nickel(III) ions magnetic interactions between A′ and B can be neglected and the magnetic susceptibility data of **1** and **2** can be analyzed using simple dinuclear approximation (the Hamiltonian being $H=2JS_AS_B$) (equation(1)) [19]:

$$\chi_M = (2N\beta^2g^2/kT)(1-\rho)/(3+\exp(-2J/kT)) + (N\beta^2g^2/2kT)\rho \qquad (1)$$

where N, g, k, β and ρ have their usual meanings, and J is the exchange coupling parameter describing the magnetic interaction between any two neighbouring $S=1/2$ spins. The parameters obtained by least-squares fit are: $g=2.12$, $J=-298.18\,cm^{-1}$, $\rho=3.0\times10^{-4}$ and $R=1.0\times10^{-6}$ for **1**, $g=2.17$, $J=-218.42\,cm^{-1}$, $\rho=9.53\times10^{-3}$ and $R=7.0\times10^{-6}$ for **2** (R is defined as $\sum((\chi_M T)^{calcd}-(\chi_M T)^{obsd})^2/\sum(((\chi_M T)^{obsd})^2)$). The low ρ values suggest that paramagnetic impurities have little effect on the magnetic measurements for **1** and **2**. The model provides an excellent fit (the solid lines figure 6a for **1** and figure 6b for **2**), as indicated by the low values of R.

4. Conclusion

Two novel ion-pair complexes [DiClBzPy][Ni(mnt)$_2$] and [DiClBzQl][Ni(mnt)$_2$] exhibiting antiferromagnetic behavior have been synthesized and their single crystal structural analyses show the $Ni(mnt)_2^-$ anion and its counter cations of complexes **1**

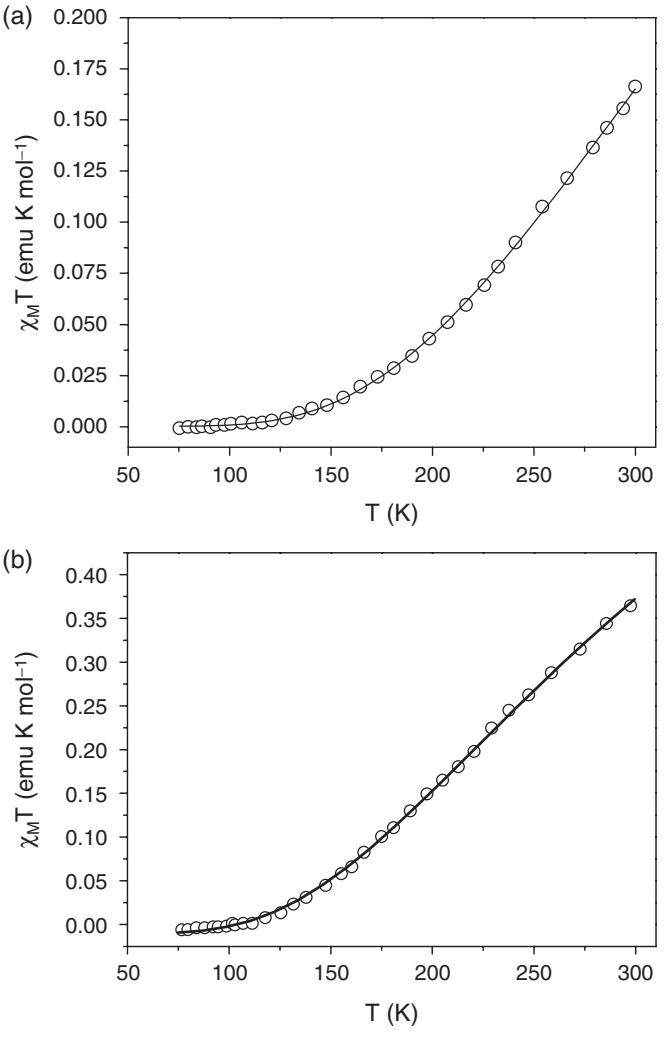

Figure 6. The plots of $\chi_M T$ *vs.* T for **1**(a) and **2**(b).

and **2** stack into well-segregated columns in the solid state. The Ni(III) ions form a 1D magnetic chain in an alternatering zigzag fashion(A–B–A′) within a $Ni(mnt)_2^-$ column through Ni···S, S···S, Ni···Ni or $\pi\cdots\pi$ interactions. As for **2**, the contacts of anion–anion, anion–cation and cation–cation play important roles in the packing and stabilization of **2**. The variable temperature magnetic susceptibilities of complexes **1** and **2** have been measured over the 75–298 K range revealing antiferromagnetic behavior with magnetic coupling of **1** is stronger than that of **2**.

Supplementary material

Supplementary crystallographic data are available from the Cambridge Crystallographic Data Center, CCDC No. 249994 and No. 249995. Copies of this

information may be obtained free of charge from The Director, CCDC, 12 Union Road, Cambridge, CB2 1EZ, UK (Fax: +44-1223-336033; E-mail: deposit@ccdc.cam.ac.uk or www: http://www.ccdc.cam.ac.uk).

Acknowledgements

We thank the president's foundation of South China Agricultural University (No. 2005K092) for financial support of this work.

References

[1] A.T. Coomber, D. Beljonne, R.H. Friend, J.L. Brédas, A. Charlton, N. Robertson, A.E. Underhill, M. Kurmoo, P. Day. *Nature*, **380**, 144 (1996).
[2] P.I. Clemenson, A.E. Underhill, M.B. Hursthouse, R.L. Short. *J. Chem. Soc., Dalton Trans.*, 1689 (1988).
[3] N. Robertson, L. Cronin. *Coord. Chem. Rev.*, **227**, 93 (2002).
[4] M. Urichi, K. Yakushi, Y. Yamashita. *J. Qin. J. Mater. Chem.*, **8**, 141 (1998).
[5] E. Canadell. *Coord. Chem. Rev.*, **185–186**, 629 (1999).
[6] J.F. Weiher, L.R. Melby, R.E. Benson. *J. Am. Chem. Soc.*, **86**, 4329 (1964).
[7] J.L. Xie, X.M. Ren, Y. Song, W.W. Zhang, W.L. Liu, C. He, Q.J. Meng. *Chem. Commun.*, 2346 (2002).
[8] J.L. Xie, X.M. Ren, C. He, Y. Song, Q.J. Meng, R.K. Kremer, Y.G. Yao. *Chem. Phys. Lett.*, **369**, 41 (2003).
[9] X.M. Ren, Q.J. Meng, Y. Song, C.L. Lu, C.J. Hu, X.Y. Chen, Z.L. Xue. *Inorg. Chem.*, **41**, 5931 (2002).
[10] X.M. Ren, Q.J. Meng, Y. Song, C.S. Lu, C.J. Hu. *Inorg. Chem.*, **41**, 5686 (2002).
[11] J.L. Xie, X.M. Ren, Y. Song, Y. Zou, Q.J. Meng. *J. Chem. Soc., Dalton Trans.*, 2868 (2002).
[12] J.L. Xie, X.M. Ren, S. Gao, W.W. Zhang, Y.Z. Li, C.S. Lu, C.L. Ni, W.L. Liu, Q.J. Meng, Y.G. Yao. *Eur. J. Inorg. Chem.*, 2393 (2003).
[13] J.L. Xie, X.M. Ren, Y. Song, W.J. Tong, C.S. Lu, Y.G. Yao, Q.J. Meng. *Inorg. Chem. Commun.*, **5**, 395 (2002).
[14] S.B. Bulgarevich, D.V. Bren, D.Y. Movshovic, P. Finocchiaro, S. Failla. *J. Mol. Struct.*, **317**, 147 (1994).
[15] A. Davison, R.H. Holm. *Inorg. Synth.*, **10**, 8 (1967).
[16] *SHELXTL*, Version 5.10, *Structure Determination Software Programs*, Bruker Analytical X-ray Systems Inc. Madison, Wisconsin, USA (1997).
[17] K. Brunn, H. Endres, J. Weiss. *Z. Naturforsch*, **42B**, 1222 (1987).
[18] S.I. Shupack, E. Billig, R.J.H. Clark, R. Williams, H.B. Gray. *J. Am. Chem. Soc.*, **86**, 4594 (1964).
[19] You Song, Dunru Zhu, Kouling Zhang, Yan Xu, Chunying Duan, Xiaozeng You. *Polyhedron*, **19**, 1461 (2000).